

See discussions, stats, and author profiles for this publication at: <https://www.researchgate.net/publication/262807739>

Cell death and tissue reorganization in Rhynchosciara americana (Sciaridae: Diptera) metamorphosis and their relation to molting hormone titers. Arthr Struct Dev

ARTICLE *in* ARTHROPOD STRUCTURE & DEVELOPMENT · SEPTEMBER 2014

Impact Factor: 1.65 · DOI: 10.1016/j.asd.2014.05.001

CITATIONS

5

READS

47

6 AUTHORS, INCLUDING:



[Jonatas Bussador Do Amaral](#)

Universidade Federal de São Paulo

36 PUBLICATIONS 79 CITATIONS

[SEE PROFILE](#)



[Paula Rezende-Teixeira](#)

University of São Paulo

21 PUBLICATIONS 93 CITATIONS

[SEE PROFILE](#)



[Klaus Hartfelder](#)

University of São Paulo - Ribeirão Preto Sc...

105 PUBLICATIONS 3,923 CITATIONS

[SEE PROFILE](#)

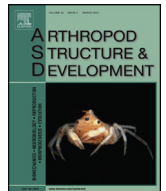


[Glaucia Maria Machado-Santelli](#)

University of São Paulo

67 PUBLICATIONS 86 CITATIONS

[SEE PROFILE](#)



Arthropod Structure & Development

journal homepage: www.elsevier.com/locate/asd

Cell death and tissue reorganization in *Rhynchosciara americana* (Sciaridae: Diptera) metamorphosis and their relation to molting hormone titers

Q8 Amanda dos Santos Brandão ^{a, b}, Jônatas Bussador do Amaral ^{a, 1, 2},
8 Paula Rezende-Teixeira ^a, Klaus Hartfelder ^c, Fábio Siviero ^a,
9 Gláucia Maria Machado-Santelli ^{a, *}

10 ^a Department of Cellular and Developmental Biology, Institute of Biomedical Sciences, University of São Paulo, Av. Prof. Lineu Prestes 1524, Ed Biomédicas 1,
11 CEP 05508-000 São Paulo, SP, Brazil

12 ^b Post-Graduate Interunits Program in Biotechnology, Av. Prof. Lineu Prestes, 2415 Edifício ICB – III – Cidade Universitária, CEP 05508-900 São Paulo,
13 SP, Brazil

14 ^c Department of Cell and Molecular Biology, Ribeirão Preto Medical School, University of São Paulo, Av. Bandeirantes 3900, CEP 14049-900 Ribeirão Preto,
15 SP, Brazil

ARTICLE INFO

Article history:

Received 10 February 2014

Received in revised form
2 May 2014

Accepted 12 May 2014

Available online xxx

Keywords:

Salivary gland
Fat body
Autophagy
Apoptosis
Postembryonic development

ABSTRACT

Programmed cell death (PCD) is a focal topic for understanding processes underlying metamorphosis in insects, especially so in holometabolous orders. During adult morphogenesis it allows for the elimination of larva-specific tissues and the reorganization of others for their functionalities in adult life. In *Rhynchosciara*, this PCD process could be classified as autophagic cell death, yet the expression of apoptosis-related genes and certain morphological aspects suggest that processes, autophagy and apoptosis may be involved. Aiming to reveal the morphological changes that salivary gland and fat body cells undergo during metamorphosis we conducted microscopy analyses to detect chromatin condensation and fragmentation, as well as alterations in the cytoplasm of late pupal tissues of *Rhynchosciara americana*. Transmission electron microscopy and confocal microscopy revealed cells in variable stages of death. By analyzing the morphological structure of the salivary gland we observed the presence of cells with autophagic vacuoles and apoptotic bodies and DNA fragmentation was confirmed with the TUNEL assay in salivary gland. The reorganization of fat body occurs with discrete detection of cell death by TUNEL assay. However, both: salivary gland histolysis and fat body reorganization occur under control of hormone ecdysone.

Published by Elsevier Ltd.

1. Introduction

Programmed cell death (PCD) is a well-known pathway to eliminate unneeded cells at some stage during development (Baehrecke, 2003; McPhee and Baehrecke, 2009; McPhee et al.,

2013). Type I PCD, or apoptosis, is characterized by bleb formation, chromatin fragmentation, and cytoplasm shrinkage. The main feature of type II PCD, autophagic cell death, is the formation of double membrane vacuoles that engulf several cellular structures and mediate their destruction. Type III PCD is a non-lysosomal type of death that is not well described (Gozuacik and Kimchi, 2004; Levine and Yuan, 2005; Orme and Meier, 2009; Liu et al., 2013).

Macroautophagy, usually referred to as autophagy, is a catabolic process that isolates unneeded cytoplasm contents into a double membrane structure known as autophagic vacuole. These autophagic vacuoles then fuse with lysosomes, forming an autolysosome. At this step, the inner vacuole membrane is also degraded. Differently from apoptosis, in this type II cell death, the chromatin and cytoskeleton are not the first targets of degradation (Cuervo, 2004; Klionsky, 2009a; Chen and Yu, 2013).

* Corresponding author. Tel.: +55 11 3091 7229.

E-mail addresses: amsbrandao@gmail.com (A. dos Santos Brandão), amaraljb@gmail.com (J.B. do Amaral), paularez@gmail.com (P. Rezende-Teixeira), klaus@fmnp.usp.br (K. Hartfelder), fsiviero@usp.br (F. Siviero), gmmsante@usp.br, glaucia.santelli@gmail.com (G.M. Machado-Santelli).

¹ Present address: Translational Research Center, ORL/CCP, Federal University of São Paulo, Rua Coronel Liboa, 958, CEP 04023-900 São Paulo, SP, Brazil.

² Present address: Santo Amaro University, Rua Professor Enéas de Siqueira Neto, 340, Jardim das Imbuias, CEP:04829-300 São Paulo, SP, Brazil.

The formation of the autophagic vacuole membrane depends on two important complexes. The Atg12-5-16 complex, which requires the Atg7 and Atg10 enzymes, participates in the elongation of the autophagic vacuole membrane. Additionally, Atg8 (mammalian LC3) receives a phosphatidyl-ethanolamine moiety and actively participates in the formation of the double membrane vacuole. LC3 (microtubule-associated protein 1 light chain 3 alpha) has been extensively used as a specific marker in different species, and its detection is believed to be the most reliable method to identify autophagic vacuoles (Klionsky, 2009b). The origin of this membrane is controversial, but some specific endoplasmic reticulum proteins found in the inner and outer autophagic vacuoles membrane are suggestive of its origin (Mizushima, 2007; Shibutani and Yoshimori, 2014). For instance, an ER-Golgi intermediate compartment was identified by Ge and Schenkman (2014). This compartment plays an essential role in triggering LC3 lipidation and autophagosome biogenesis by recruiting the key early autophagic factor ATG14 (Ge and Schenkman, 2014).

Denton et al. (2010) demonstrated that specific autophagic features are present during the elimination of different tissues in *Drosophila*. Autophagy markers could be detected during the early events of histolysis, but apoptotic features and genes, including apoptotic suppressors, were also seen to cooperate in this process. Certain caspases take part in autophagic cell death, yet in some cases, the knockout of these proteins could only retard cell death in salivary glands, but did not block the histolysis process (Berry and Baehrecke, 2007; 2008; Tracy and Baehrecke, 2013). Furthermore, the PCD type seen within the same biological model can depend on the tissue being studied. In *Drosophila*, caspases are known to cooperate with autophagy in the destruction of salivary glands and fat body, but did not interfere in midgut histolysis, resulting in an autophagy-only pathway in this tissue (Denton et al., 2009, 2010).

Hou et al. (2008) demonstrated that the IAP protein family Bruce inhibits autophagy in the *Drosophila* ovary, and the effector caspase Dcp-1 and the autophagy genes Atg1 and Atg7 are essential for successful cell death in this tissue. In *Drosophila melanogaster* Dark (Apaf-1 homolog) mutants, the salivary gland persisted intact until 36 h after puparium formation, although autolysosomes were identified in these mutants (Akdemir et al., 2006). Another important regulator of cell death in insects is the molting hormone 20-hydroxyecdysone (ecdysone), which presents specific peaks during development and regulates the passage through the post-embryonic phases (Borst et al., 1974; Hodgetts et al., 1977). Nevertheless, some cell death-related genes do not seem to be regulated by this hormone, such as the tumor suppressor Wts in *Drosophila* (Martin et al., 2007).

The fungus gnat genus *Rhynchosciara* has been the subject of decades of research, particularly with regard to puff formation in salivary gland polytene chromosomes and gene amplification (Pavan and Breuer, 1952; Machado-Santelli and Basile, 1975; Winter et al., 1977a,b; Santelli et al., 1991, 2004; Rezende-Teixeira et al., 2012). An EST library constructed from *Rhynchosciara americana* salivary gland tissue during the spinning of the communal cocoon in the last polytene DNA replication cycle revealed several different transcripts, including anti-apoptotic putative genes such as Dad-1, Bax-inhibitor-1 and IAP-1 (Siviero et al., 2006). The salivary glands, which are believed to play a central role in the construction of the communal cocoon, undergo cell death during metamorphosis.

The fat body presents another complex model of cell death in many insects. The fat body, a tissue with great metabolic and biosynthetic activity, is the center of the insect intermediary metabolism (Keeley, 1985; Law and Wells, 1989). This tissue undergoes extensive cell death during metamorphosis. Nonetheless, as shown by Aguila et al. (2007) some GFP-expressing larval fat

body cells were still present in adult fruit flies, suggesting that these floating fat body cells are an important nutrient source in the early days of adult life.

These tissue remodeling processes during metamorphosis are synchronized by steroid hormones, the ecdysteroids. Ecdysteroids, especially so 20-hydroxyecdysone play a crucial role in the biology of insects, regulating molting and the metamorphosis processes, as well as reproductive events (Nijhout, 1984; Riddiford et al., 2003). In *D. melanogaster*, ecdysteroids are released by the ring gland in distinct peaks during development, and these peaks were shown to coincide with the triggering of salivary gland histolysis (Lee and Baehrecke, 2001) and the reorganization of the fat body.

We herein investigated the ultrastructural, apoptotic and autophagic features of the salivary glands and the fat body during *R. americana* development in order to understand the programmed cell death pathway in *R. americana* and whether and how these contribute to tissue reorganization during metamorphosis. There are several advantages to studying these processes in *R. americana* larvae and pupae as they are naturally of the same sex and synchronous in their development once they gather in a communal cocoon. Furthermore, they are rather slow developers, compared to *Drosophila*, which makes it easier to track changes related to cell death and tissue reorganization on an expanded time scale. These characteristics have already greatly contributed to establish a precise time scale in metamorphosis-related gene activation patterns making these fungus gnats an interesting non-model organism for insect metamorphosis.

2. Materials and methods

2.1. Animals

Larvae of *R. americana* were collected at field sites in the region of Ubatuba, State of São Paulo, Brazil, and bred in the laboratory under the conditions established by Lara et al. (1965).

R. americana development lasts approximately sixty days, and the pupal period is approximately 8–10 days. Larval development is divided into four instars, of which the fourth is the longest and is subdivided into six periods. At the end of the fourth instar, the communal cocoon is built and metamorphosis then occurs synchronically (Breuer and Pavan, 1955; Terra et al., 1973). The following developmental stages were used in the cytological studies and for ecdysteroid titer analyses: all periods of the fourth instar larval (1P–6P), prepupal stage and six days of pupal development.

2.2. Stereomicroscopy and light microscopy (cytological preparations)

Salivary glands and fat bodies were dissected in PBS (140 mM NaCl, 2.7 mM KCl, 1.5 mM KH₂PO₄, 6.5 mM Na₂HPO₄) and immediately photographed under a stereomicroscope (Leica). After fixation in ethanol-acetic acid (3:1), the chromosomes or tissues were stained with acetic orcein or hematoxylin/eosin and images were taken on a Zeiss microscope equipped with an AxioCam.system (Zeiss).

2.3. TUNEL (Terminal deoxynucleotidyl transferase biotin-dUTP nick end labeling)

Salivary glands and fat body tissues dissected in PBS were fixed for 5 min with 3.7% formaldehyde. After treatment with 1% Triton X-100 for 10 min, the TUNEL reaction was performed by means of an In Situ Cell Death Detection kit, TMR red (Roche), following the

manufacturer's instructions. Images were acquired with a confocal laser scanning microscope (Zeiss LSM 510).

2.4. Immunofluorescence

Formaldehyde-fixed tissues treated with 1% Triton X-100 in PBS for 10 min, were blocked with PBS containing 1% bovine albumin for 1 h and washed with PBS. They were incubated with an LC3-specific primary antibody generated in rabbit (anti-LC3, Abcam) diluted 1:500 overnight. After three washes with PBS they were incubated for 2 h with a secondary goat anti-rabbit IgG antibody labeled with FITC (Sigma—Aldrich), diluted 1:200 in PBS. The nuclei were counterstained with propidium iodide for 10 min. In control slides, the primary antibody was omitted (data not shown).

The actin cytoskeleton was visualized by means of staining with FITC-phalloidin (Sigma) for 1 h, after the fat body was treated with RNAase (Sigma—Aldrich) for 20 min, and the nuclei were counterstained with propidium iodide.

Laser scanning confocal images were acquired in a LSM 510 (Zeiss) microscope using the Argon green (458, 488, and 514 nm), Helium—Neon 1 (543 nm), and Helium—Neon 2 (633 nm) lasers. Optical slices were obtained at adequate intervals along the Z axis (between 0.5 and 1 μm width). Different modules of the LSM 510 3D software (Carl Zeiss) were used in confocal image analysis, including slice projections.

2.5. Monodansylcadaverine (MDC)

The pupae were dissected in Grace's medium (Sigma—Aldrich) and the salivary gland incubated for 30 min with 1 μM MDC (Sigma—Aldrich) ex vivo. After fixation in 3.7% formaldehyde for 5 min, the tissues were treated with RNAase (Sigma—Aldrich) for 30 min, and the nuclei were counterstained with propidium iodide, as mentioned above. Images were acquired with a confocal laser scanning microscope (Zeiss LSM 510).

2.6. Transmission electron microscopy

Salivary glands and fat body cells were dissected and fixed for 2 h with 2.5% glutaraldehyde and 2% formaldehyde in 0.1 M sodium cacodylate buffer (pH 7.2). The fixed samples were washed in 0.1 M sodium cacodylate buffer (pH 7.2) and post-fixed in 1% osmium tetroxide in the same buffer. The tissues were dehydrated in a graded ethanol and propylene oxide series. Resin infiltration was done with a 1:1 mixture of propylene oxide and EPON (Electron Microscopy Science, PA, USA) for 5 h, followed by pure Epon for another 5 h. Next, the material was embedded in Epon and polymerized for 48 h. Thin sections were cut using an ultramicrotome and stained with toluidine blue or hematoxylin/eosin. Appropriate regions of the salivary glands and fat body were then thin-sectioned at 70–90 nm and stained with 4% uranyl acetate and a 10% lead citrate solution. The material was analyzed with a Jeol 1010 transmission electron microscope at 80 kV.

2.7. Hemolymph sampling and ecdysteroid titer measurement

Hemolymph was collected from punctured animals at different developmental ages by using a micropipette. Ecdysteroids were extracted from hemolymph by the addition of a 100-fold volume of cold methanol (-20°C). The precipitate forming at 4°C within at least 1 h was removed by centrifugation (14,000 g at 4°C for 10 min). Aliquots of the supernatant were transferred to 1 ml glass vials, and the solvent evaporated by vacuum centrifugation (Speed-VacPlus SC110A, Savant). The ecdysteroids were quantified by radioimmunoassay (Feldlaufer and Hartfelder, 1997; Araujo et al.,

2011), using an antiserum prepared against a hemisuccinate derivative of ecdysone (Warren and Gilbert, 1986; Bollenbacher et al., 1983) at a final concentration of 0.05%. [23, 24-3H (N)] ecdysone (NEN, specific activity 102 Ci/mmol) served as labeled ligand. As standard curves were set up using 20-hydroxyecdysone (20E, Simes, Milan) as non-radioactive ligand, all ecdysteroid titer results are expressed as 20E equivalents (pg/ μl hemolymph).

3. Results

3.1. Salivary gland: morphological aspects, apoptotic and autophagic features of cell death

Larval salivary glands exhibit a characteristic morphology comprising three distinct regions: S1, S2, S3 (Fig. 1, Column A). According to Pavan (1965) ... "for practical purposes the salivary gland is divided in three regions: S1, S2 and S3. S1 corresponds to the proximal quarter of the gland, where there are only two opposite rows of rather thick cells enveloping the lumen of the gland. S2 includes the 2nd and 3rd quarters of the gland; the lumen normally has a larger diameter in this region and is surrounded by a single layer of flat cells. S3 correspond to the last quarter of the gland, where the lumen is surrounded by a double row of cells distributed in an alternating pattern." During larval development, cells are organized around a well-delineated luminal space and after the cocoon secretion, it is possible to observe that the luminal space shrinks in young pupae (Fig. 1, Column B). The salivary glands start to modify their morphology from 1–2 to 4–6 days-old pupae. The gland contour becomes irregular showing cells protruding when observed under a stereomicroscope (Fig. 1, Columns A and B). In salivary glands of older pupae (4/5 days-old pupa), the acetic orcein staining revealed both normal nuclei with intact polytene chromosomes and apoptotic ones (Fig. 1, Column C – arrowhead and asterisks, respectively).

As the acetic orcein staining indicated the occurrence of fragmentation of nuclei we further investigated this typical apoptotic signal by means of a TUNEL assay (terminal deoxynucleotidyl transferase biotin-dUTP nick end labeling) in *R. americana* salivary gland cells during the pupae period. TUNEL-positive nuclei confirmed DNA fragmentation in some cells, while neighboring ones were negative, indicating that they were intact (Fig. 2, upper row). Compared with larval salivary glands (Fig. S1A), only the pupal salivary glands presented TUNEL-positive nuclei. These results put in evidence that apoptotic features contribute to PCD in *R. americana* salivary glands, and even at the late stage of their disintegration we continued to observe dying cells at different stages.

To see whether autophagy was occurring concomitantly with apoptotic cell death we investigated the presence of autophagic vacuoles in pupal salivary glands of *R. americana*. To this end we performed assays with two specific autophagosome markers: an antibody against LC3-II and monodansylcadaverine (MDC), both being specific markers of autophagic vacuoles (Niemann et al., 2000, 2001; Klionsky et al., 2009b). In the pupal salivary glands stained with the fluorescent dye MDC we observed spherical structures surrounding condensed nuclei (Fig. 2, middle row).

Compared with salivary glands from young larvae (Fig. S1B), only the pupal salivary glands presented MDC labeled cells. Immunofluorescence imaging with the anti-LC3 antibody revealed punctate labeling in the pupal salivary gland, indicating the presence of LC3-II in the cytoplasm of cells already at an early stage of cell death, as in some of the positive LC3 cells polytene chromosomes were still present (Fig. 2, bottom row). The lack of positive LC3 cells in larval salivary gland indicate that the labeling is only in the pupal salivary gland (Fig. S1C).

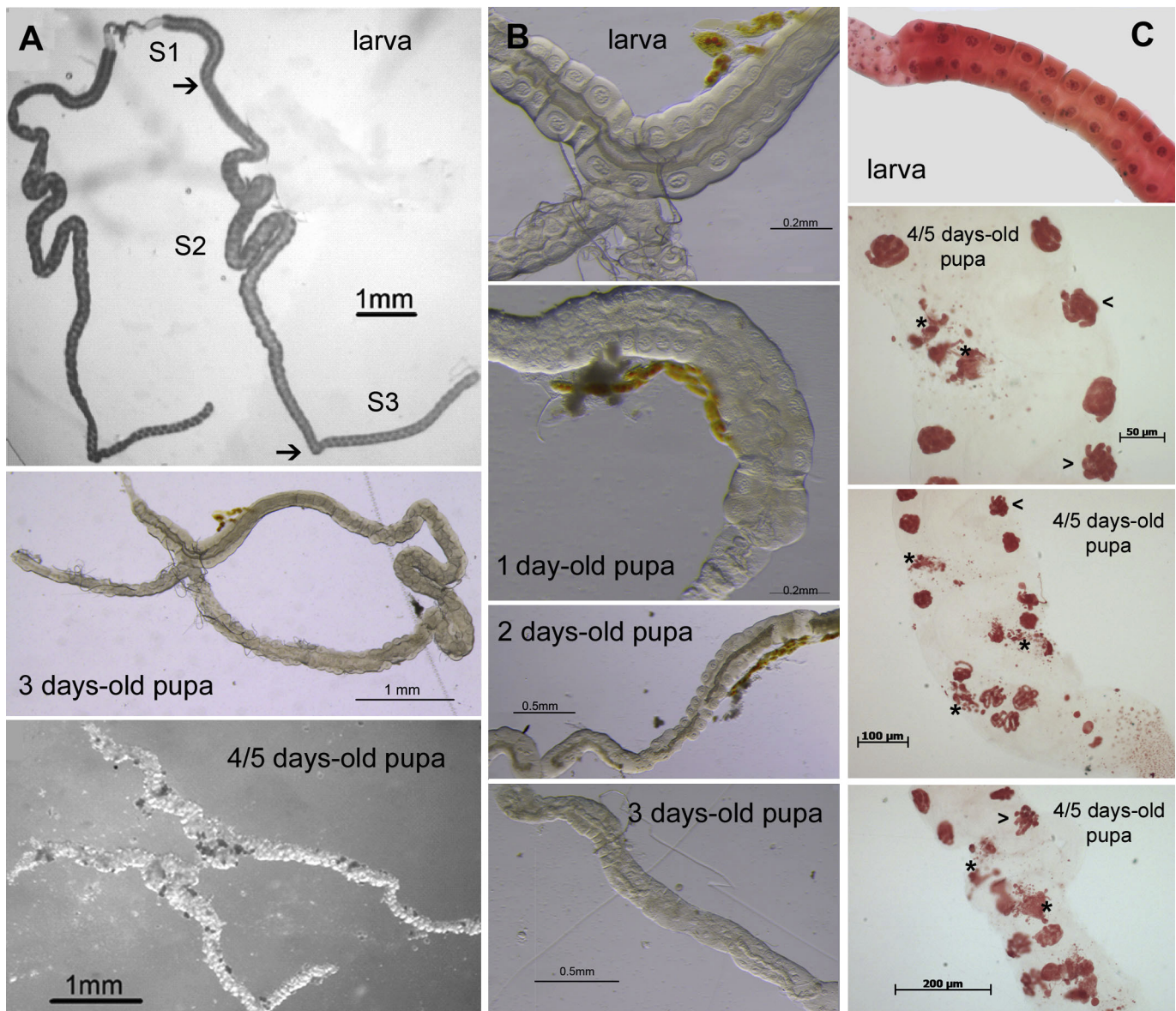


Fig. 1. Salivary gland morphology: Column A shows stereomicroscopy images of larval salivary gland (regions S1, S2 and S3 are indicated and separated by arrows), the middle one is the image of a 3-days-old pupa showing the initial morphological alterations, and the last image is a salivary gland of 4/5-days old pupa; Column B: S1 region of salivary gland images in high magnification, from the top to the bottom, larva, 1day, 2days and 3 days-old pupae; Column C shows images obtained by light microscopy of salivary glands stained with acetic orcein; the upper one is from larval salivary glands, followed by a series taken from 4/5 days-old pupae. Asterisks show apoptotic nuclei, and arrowhead show intact nuclei.

Transmission electron microscopy images of *R. americana* salivary glands, in third period of fourth instar larval, showed that the cells are polarized, with the apical region facing the duct lumen. The apical surface of the cells presented abundant microvilli (MV) and secretion. At this surface, we also observed the presence of electron dense material, corresponding to the cuticle (Ct), which has only a few fenestrae to the lumen, and where some residual secretion was seen (Fig. 3A). The presence of a well-developed rough endoplasmic reticulum is suggestive of intense protein synthesis (Fig. S1D) is combined with vesicle traffic in the microvilli (detail in Fig. 3A1). In the basal region of the secretory cells, the plasma membrane presented several invaginations subjacent to the basal lamina (Lb). A large number of mitochondria (M) were observed in this region (Fig. 3B). During salivary gland histolysis following cocoon formation we observed considerable changes in cell content and morphology. In the pupal salivary gland cells (4

days-old pupa), the basal lamina appeared retracted and the basal membrane showed several invaginations (Fig. 3C). In the pupal salivary glands, the cytoplasm contained numerous distinct types of vacuoles, and at this stage the nucleus was more electron dense (Fig. 3C).

In the cytoplasm, we observed different types of vacuoles. There were double membrane vacuoles that may be associated with different stages of the gland degradation process (Fig. 3D–E). Several different types of organelle remnants were observed inside these vacuoles, including rough endoplasmic reticulum (Fig. 3E), this indicating the formation of autophagosomes.

3.2. Fat body: morphological aspects and apoptotic cell death

During the larval stage, the fat body has a typical sheet-like morphology (Fig. 4A, Larva), but during metamorphosis, tissue

1 Salivary Gland

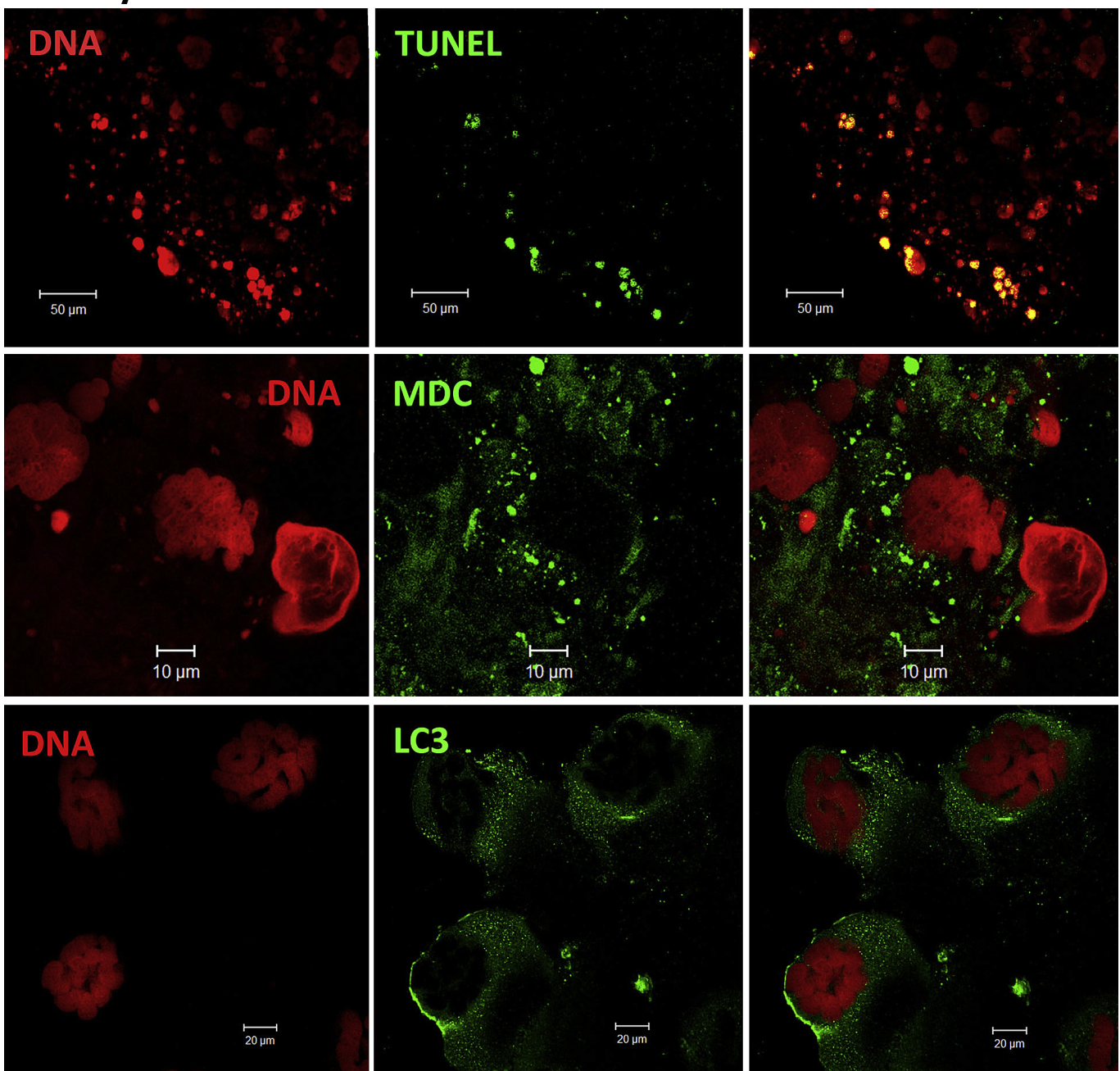


Fig. 2. Laser scanning confocal microscopy images of salivary gland of 4/5 days-old pupae evidencing cell death markers: TUNEL reaction (terminal deoxynucleotidyl transferase biotin-dUTP) staining performed in pupal salivary glands demonstrates DNA fragmentation. Monodansylcadaverine staining (MDC) (green) shows autophagic vacuole formation during the pupal stage. Immunofluorescence reaction with anti-LC3 antibody of pupal salivary glands presents punctate staining. Nuclei were counterstained with propidium iodide. The last column presents merged images of the two prior ones.

organization is completely modified. The larval fat body cells disaggregate and reorganize into small clusters floating in the hemolymph (Fig. 4A and 1d pupae – 3d pupae). These cells are also present in adult flies, however in smaller number. The actin cytoskeleton reorganizes during this tissue remodeling process. In larval fat body, actin cytoskeleton is uniformly distributed, and during the tissue remodeling the microfilaments concentrate in the cellular cortex, meanwhile the tissue is remodeled from sheet-like for clusters of cells (Fig. 4B and Fig. S2). The TUNEL reaction was used to further investigate cell death in fat body cells during the

pupal period of *R. americana* development. A few TUNEL-positive nuclei were observed indicating DNA fragmentation, an apoptosis feature, as part of the fat body remodeling process in the early stages of pupal development (Fig. 5). However, most of the fat body cells persisted until the adult phase. Compared with larval fat body (Fig. S3A), only the pupal fat body presented TUNEL-positive nuclei.

The ultrastructure analysis of pupal fat body cells revealed morphological heterogeneity among endocytotic vesicles (Fig. 6A and B). Different types of vesicles were present in these cells, including homogeneous electron dense and electron dense vesicles

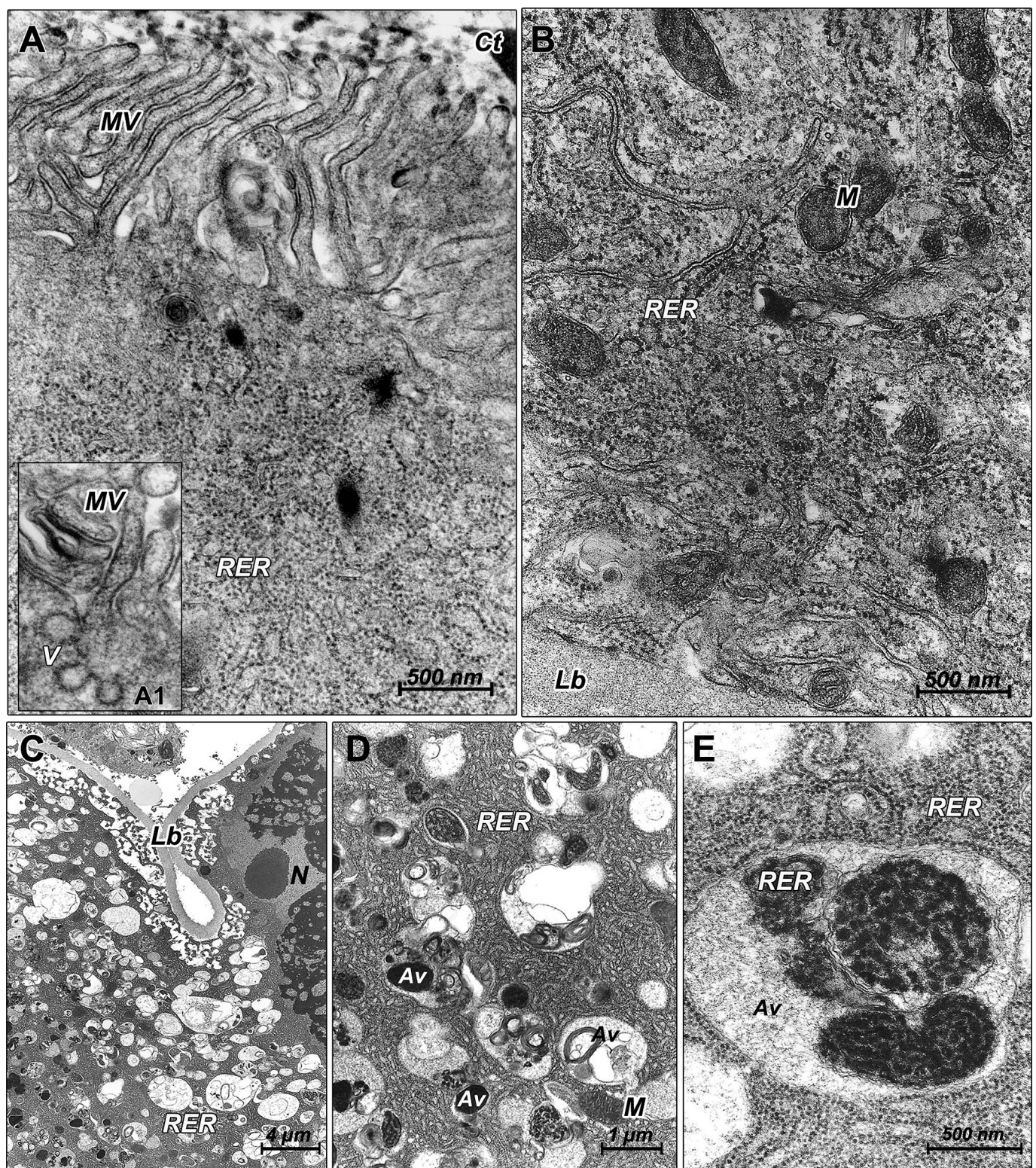


Fig. 3. Salivary gland ultrastructure during different development stages: A – larval salivary glands during construction of the communal cocoon show cytoplasm with large amounts of rough endoplasmic reticulum (RER), apical region microvilli (MV) and a cuticle (Ct). There is also evidence for vesicle (V) traffic in the basal microvilli region (A1 detail). B – In the basal region of larval salivary glands, several mitochondria (M) were observed near the basal lamina (Lb). C – Low magnification of pupal salivary gland cells (4 days-old pupa), showing vacuole distribution, the presence of invagination of the basement membrane (Lb) and the highly condensed nucleus (N). D – Pupal salivary gland (4 days-old pupa) cytoplasm containing large amounts of rough endoplasmic reticulum (RER) and autophagic vacuoles (Av) in different stages of degradation. E – Autophagic vacuole (Av) with the rough endoplasmic reticulum (RER) shown in detail during the degradation process in 4 days-old pupa.

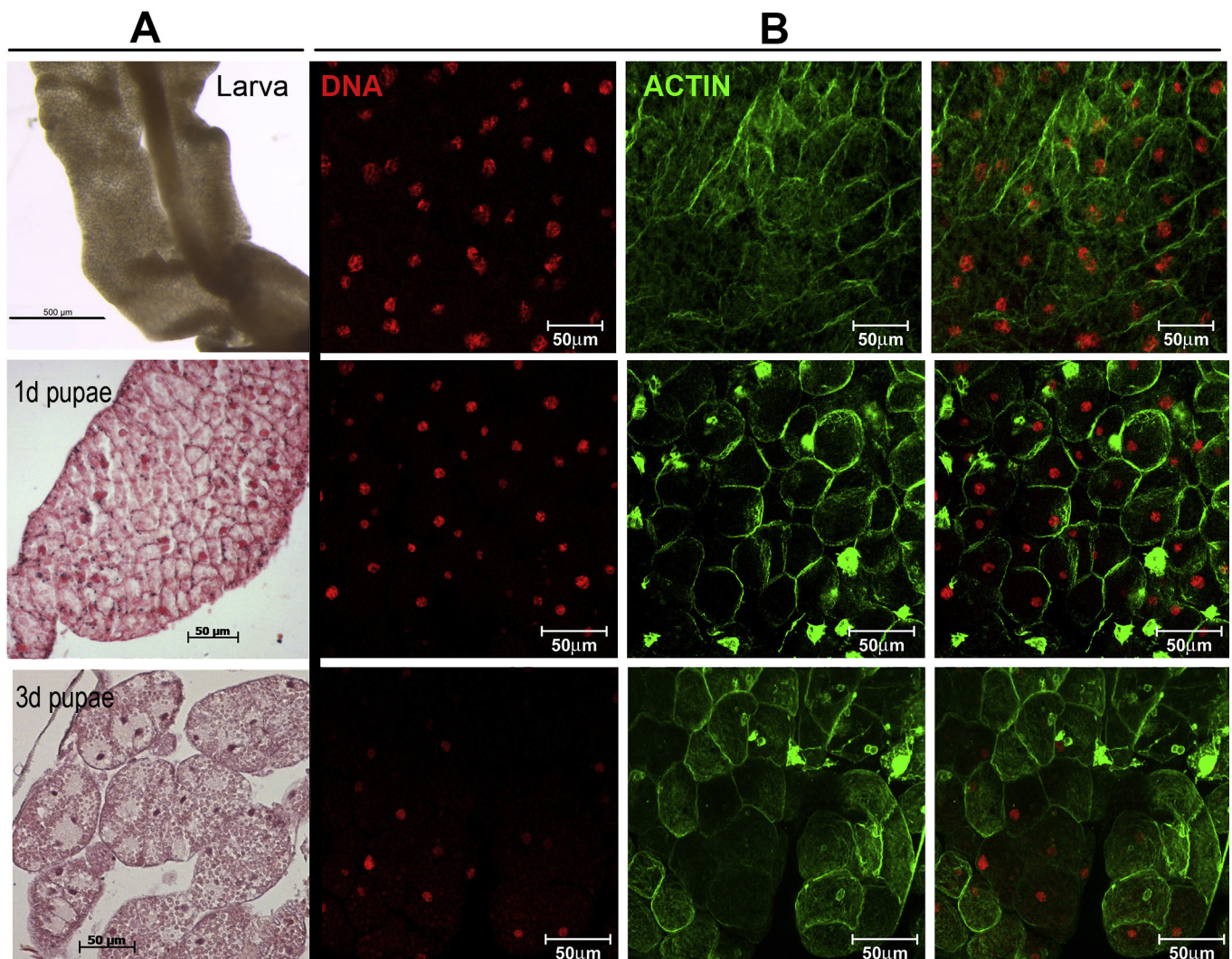


Fig. 4. Fat Body Morphology: Panel A) stereomicroscope image of larval fat body morphology (top) and histological preparations (hematoxylin & eosin stained) from 1 day old and 3 days old pupae; Panel B) laser scanning confocal microscope images of *R. americana* fat body stained with FITC-phalloidin (green) and propidium iodide (red): upper row – larva; middle row – 1 day-old pupa; bottom row – 3 days-old pupa.

presenting several tiny electron lucid regions within (Fig. 6A, B). In details (Fig. 6A1), an electron dense vesicle with a double membrane is shown engulfing cytoplasm contents. The vesicles associated with such small electron lucid structures are suggestive of autolysosomes (Fig. 6B).

In the adult fat body, the electron dense vesicles with electron lucid structures were the most prevalent ones (Fig. 6C). At higher magnification (Fig. 6D) we also observed the presence of abundant mitochondria in the fat body cells of these fungus gnats. In the meantime, the larval fat body ultrastructure shows homogeneous electron dense vesicles and lipid droplets (Fig. S3B), reinforcing that the heterogeneous vesicles observed in pupal fat body would correspond to autophagic process.

3.3. Hemolymphecdysteroid levels during metamorphosis

The ecdysteroid titers in *R. americana* fourth instar larvae and pupae were measured by radioimmunoassay to assess their possible role in the death/reorganization processes of the tissues studied in this work. The ecdysteroid hormone profile (Fig. 7) showed two hormone peaks. The first peak occurring before the prepupal stage represents a steep rise from low titer levels prior to

the onset of metamorphosis. This peak is concomitant with the onset of salivary gland histolysis and preparation for the pupal molt. The second, higher peak of ecdysone hormone seen in four day-old pupae coincides with the reorganization of the fat body and the final steps of salivary gland histolysis. This temporal correlation indicates that, like in *Drosophila*, ecdysteroids also play an important role in *R. americana*, in synchronizing characteristic events of cell death and tissue reorganization during metamorphosis.

4. Discussion

4.1. Salivary gland degradation

In the present study, we focused on the cell death and tissue remodeling in *R. americana* salivary gland and fat body, tissues with different functions during insect development. Differently from *Drosophila*, *R. americana* metamorphosis encompasses a long period, and so, tissue remodeling occurs over several days. By the end of larval life, the salivary glands participate in the construction of a communal cocoon and, thereafter, have no more functions in metamorphosis or adult life. The histolysis process typically lasts

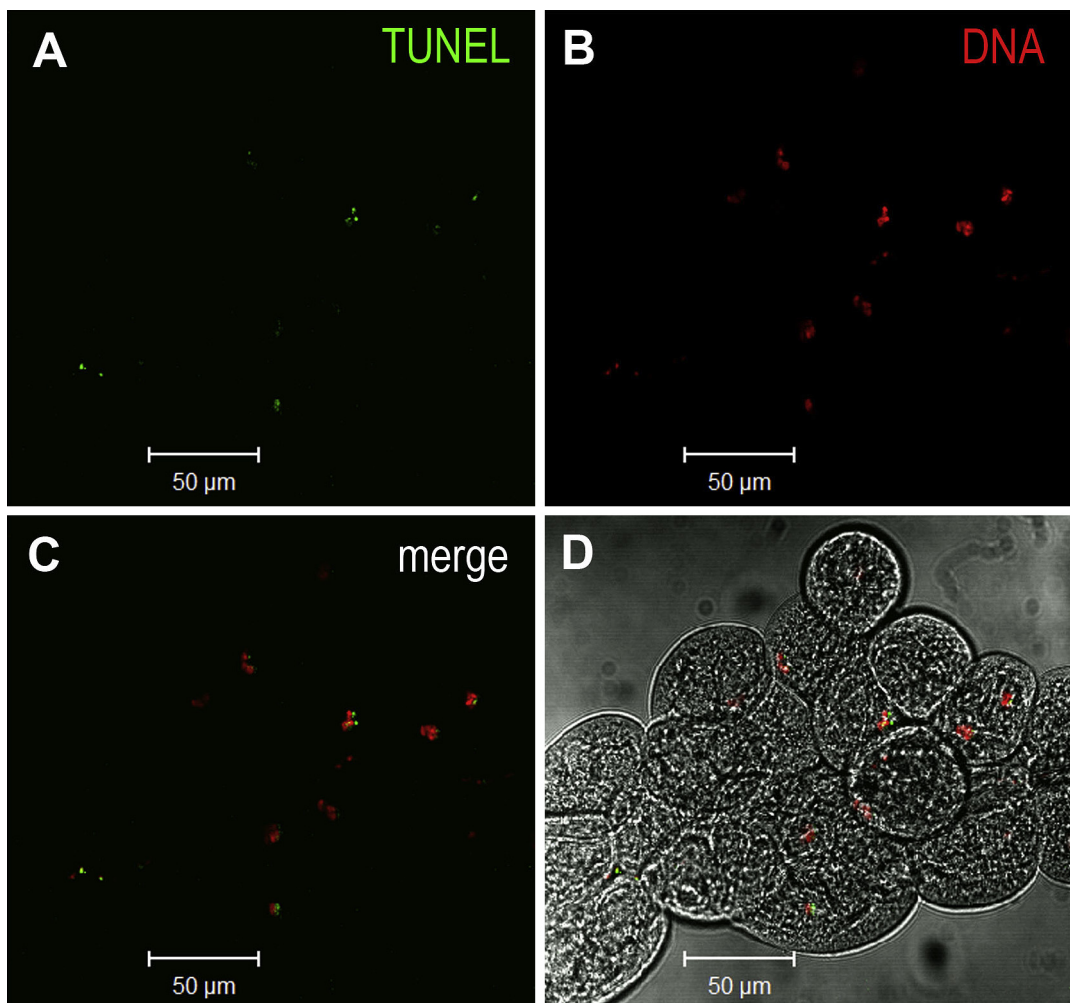


Fig. 5. Laser scanning confocal microscopy images of pupal fat body submitted to TUNEL reaction (green) showing some double-labeled nuclei: A) TUNEL reaction (terminal deoxynucleotidyl transferase biotin-dUTP), B) DNA stained nuclei, C) merged images; D) Fluorescence channels + DIC image, evidencing fat body fragmentation. (For interpretation of the references to colour in this figure legend, the reader is referred to the web version of this article.)

for at least five days during the initial pupal phase. Already shortly after the ecdysone peak associated with the pupal molt, gross changes in gland morphology occurred, followed by clear signs of cell death. As such we found DNA and chromatin fragmentation in *R. americana* salivary glands to occur concomitantly or just right before signs of autophagy were denoted. The histolysis mechanism we observed is similar to that seen in salivary glands of other Diptera. In *Drosophila* salivary gland histolysis, both caspase activation and autophagic vacuole formation were observed (Aguila et al., 2007; Berry and Baehrecke, 2007; Qu et al., 2007).

Such vacuoles were abundant in *R. americana* salivary glands during the pupal period, indicating that vacuole formation takes place during the histolysis process. To confirm this we analyzed late fourth instar larvae as controls, and we did not observe MDC labeling in these. Autophagic vacuole formation in the salivary glands was further confirmed by immunofluorescence reaction with an anti-LC3 polyclonal antibody. This revealed the presence of numerous punctate aggregates of LC3 protein, suggesting that the formation of such vacuoles starts with double membrane formation. As described earlier, the punctate labeling corresponds to LC3 conjugated with phosphatidyl-ethanolamine, forming LC3-II. Under non-autophagic conditions, LC3-I is diffusely distributed throughout the cytoplasm (Mizushima, 2007; Hannigan and Gorski, 2009; Rubinsztein et al., 2009). Our immunofluorescence

results are, thus, consistent with the ultrastructure analyses, showing that the vacuoles found in the tissue are in fact autophagic and participate in the intense degradative activity that occurs during elimination of the salivary glands.

Since autophagy seems to be associated with both cell death (salivary glands) or survival (fat body reorganization), Berry and Baehrecke (2008) proposed that autophagy may be responsible for providing energy used in corpse removal, or that it participates in this process directly, since no phagocytes were observed. Time lapse studies of *Drosophila* salivary glands kept in short term cultures enabled the observation of autophagic degeneration, as well as an ecdysone-related induction of DNA fragmentation, thus confirming the participation of the two PCD features in fly salivary gland histolysis (Myohara, 2004). Although *R. americana* has the advantage of synchrony of the metamorphic animals in a cocoon, such short term cultures would not be feasible due to the long duration of the histolysis process.

Ultrastructure analysis of *Rhynchosciara* salivary glands during the larval period showed that these cells are committed with intense protein synthesis, which involves the construction of the communal cocoon (Winter et al., 1977a, 1977b). Both the presence of cytoplasm filled with rough endoplasmic reticulum (RER) and abundant microvilli in the apical region of the gland cells indicate that this tissue has substantial importance in metamorphosis of these flies.

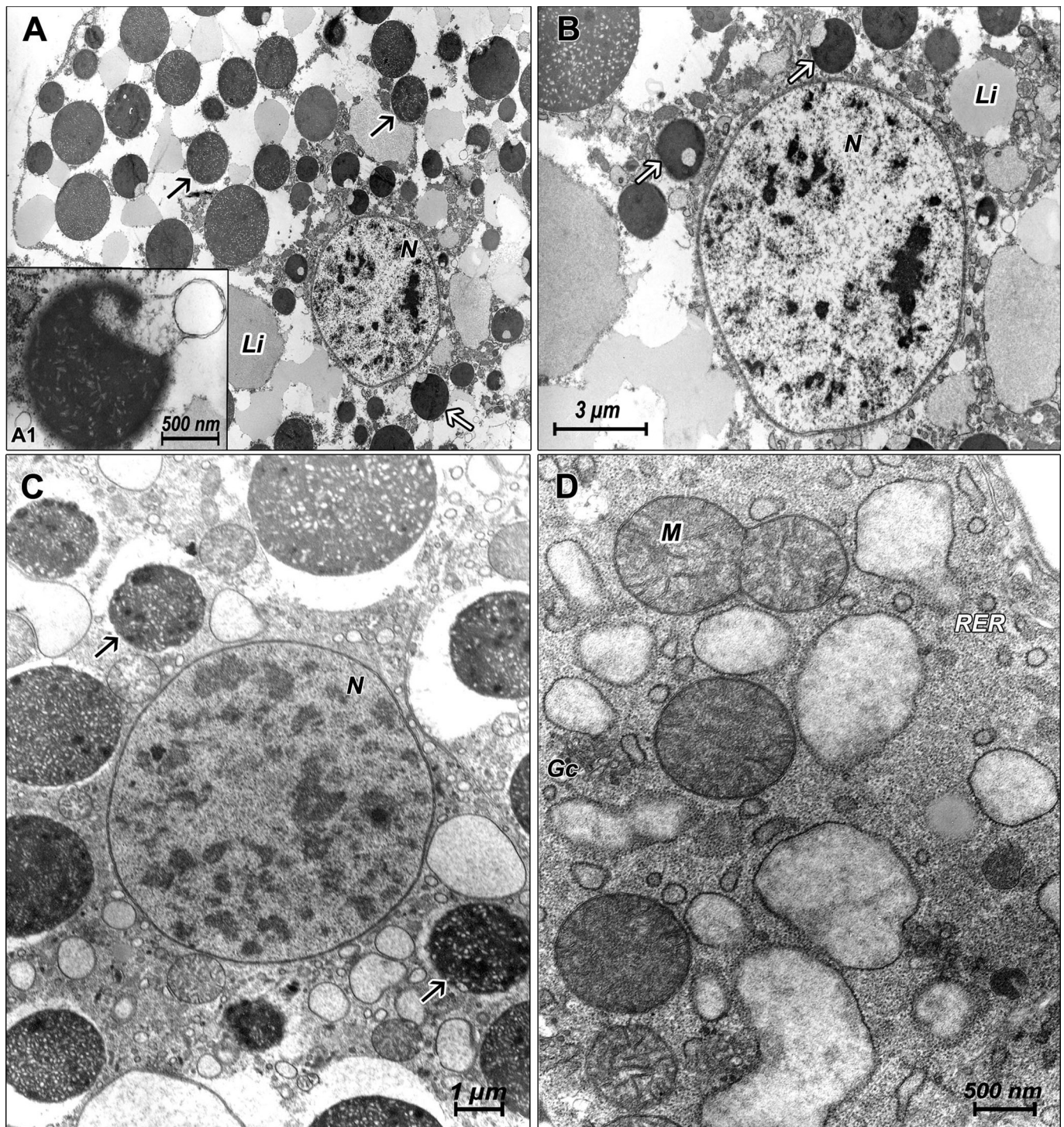


Fig. 6. Pupal and adult fat body cells shown by transmission electronic microscopy. A – Pupal fat body cells present distinct structures, such as electron dense vesicles with multiple granules (black arrow), electron dense vesicles with electron lucid fragments (white arrow) and lipid droplets (Li). In (A1), an electron dense vesicle with a double membrane is shown engulfing cytoplasm contents. N = nucleus. B – Pupal fat body nucleus in detail and electron dense vesicles with electron lucid fragments (white arrow). C – Adult fat body cells predominantly present vesicles of heterogeneous ultrastructure (black arrow). D – Detailed image of adult fat body cells showing mitochondria (M), Golgi complex (Gc) and rough endoplasmic reticulum (RER).

Similar ultrastructure analyses performed previously in *Rhynchosciara hollaenderi* salivary glands by Jurand and Pavan (1975) describe early signals of vacuole formation during puff 2B activity (which occurs at 4th period, 4th larval instar), and these autophagic activities persisted until the pupal stage. These observations differ from ours on *R. americana*, where the onset of autophagic vacuole formation coincided with the prepupal period. Possibly, the earlier

autophagic vacuole formation seen in *R. hollaenderi* may have been associated to some degree of larval starvation.

4.2. Fat body reorganization

Fat body cells are the center stage of the insects' intermediate metabolism, not only during and after feeding bouts, but also in

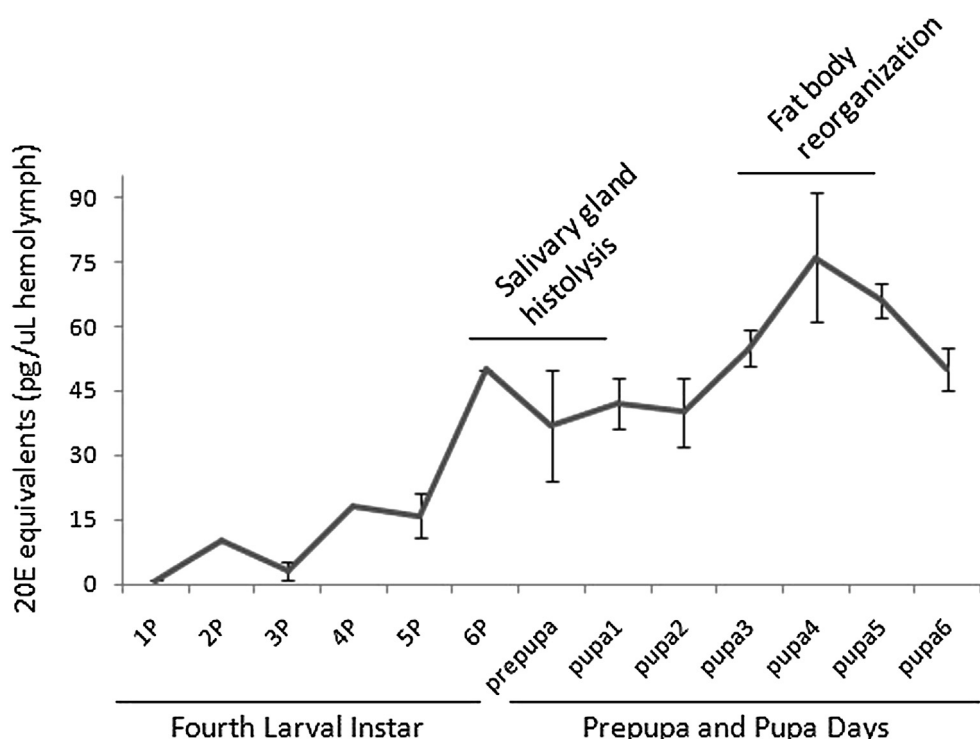


Fig. 7. Hemolymph ecdysteroid titer in last instar larvae and pupae of *Rhynchosciara americana*. Hemolymph sampled from six time points in the larval fourth instar (1P – 6P), from prepupae and during the first six days of pupal development (pupa1 – pupa6) was analyzed by radioimmunoassay with 20 hydroxyecdysone (20E) as non-labeled ligand for standard curves. Titer values are, thus, expressed as 20E equivalents. During the fourth instar, the titer levels showed a gradual increase and reached a first peak just before prepupa formation. They remained at a plateau during the prepupal stage and the first two pupal days, before rising to the second, very pronounced pupal peak, which was reached on day 4. The subsequent decline already represents the transition for the preparation of the adult molt. Titer levels are means \pm S.E.M. for 5 larvae per stage. The graph also shows the cell death and tissue reorganization events associated with the respective hemolymph ecdysteroid titer.

nutrient mobilization in non-feeding periods of the adult life cycle (Aguila et al., 2007). The typical sheet-like morphology of the larval fat body disassociates during the pupal period, and accompanying this process we observed DNA fragmentation in some fat body cells indicative of cell death associated with the ecdysone peak triggering the pupal molt in *R. americana*.

Fat body cells are considered refractory to cell death in some insects. In *Drosophila* however, apoptosis events were seen to gradually increase in fat body during the larval–pupal transition, accompanying the increase in ecdysone levels (Liu et al., 2009). Also in the silkworm, *Bombyx mori*, some fat body cells are eliminated by apoptosis during the pupal molt, and apoptotic genes are up-regulated by ecdysone (Tian et al., 2012).

In *R. americana*, fat cells detached from each other in 4–5 days-old pupae, when a higher titer of ecdysone was detected. Currently we do not know whether this represents a direct or indirect ecdysone effect. Lindmo et al. (2006) demonstrated for instance that ecdysone down-regulated the PI3K signaling pathway, which is involved in autophagy suppression in *Drosophila*.

Differently from *Drosophila*, the fat body remodeling process in *R. americana* is slow and results in the formation of cell clusters with a reorganized actin cytoskeleton. Observations of the cytoskeleton in the fat body demonstrated the changes occurring during tissue remodeling, indicating its importance in autophagic process (Bursch et al., 2000).

Some larval fat body cells can still be found in young adult flies but rapidly disappear during their 7–8 days of life. Aguila et al. (2007) presented evidence that floating fat body cells in adult fruit flies were derived from larval cells that persisted throughout the adult stage and that by inhibiting the cell death pathway, adult resistance to starvation was increased. Fat tissue dissociation has

been observed and described in detail in several insect species, including *Drosophila*, *Sarcophaga*, *Calpodes* and others, and is considered a typical aspect of the metamorphosis process of holometabolous insect (Hoshizaki, 2005; Nelliot et al., 2006).

The pupal fat body cells of *R. americana* present at least two different types of vesicles in their cytoplasm: one is electron dense and the other is associated with electron lucid fragments. Based on this observation we assume that these distinct types represent different stages of the degradation process occurring in autophagic vacuoles. MDC labeling or immunofluorescence reaction with anti-LC3 polyclonal antibody failed in evidencing positive autophagic structures in both: larval and pupal fat body (Fig. S3C–F), in spite of the ultrastructure results. Autophagy is a catabolic process that can function in both cell death and cell survival, and it has been the object of study in several fields, such as degenerative disease, aging and immunity (McPhee and Baehrecke, 2009). Several mechanisms are involved in this process. The *atg* genes (autophagic related genes), first identified in yeast, and growth arrest are required for cell death, but in some cases, the knockout of caspase gene functions is able to retard, but not prevent, cell death (Berry and Baehrecke, 2007; Berry and Baehrecke, 2008).

Based on our findings, the programmed cell death events seen in *R. americana* salivary glands and fat body predominantly showed characteristic features of autophagic cell death, but these were frequently also accompanied or followed by DNA fragmentation, characterizing the apoptotic pathway. Thus, multiple types of programmed cell death contribute to metamorphosis in this insect within the same tissue. Furthermore, while cell death leads to the complete removal of the larval salivary glands, this is not the case for the larval fat body, where groups of cells change their neighborhood characteristics and become floating groups that can

survive and function until the early adult stage. At least in the insect fat body, autophagy is associated with cellular remodeling and, thus, would not represent a PCD pathway in the strict sense, but could have consequences in macromolecule and energy recycling and even aging.

Uncited reference

Q7 Basso et al., 2002, Burry, 2000, Martin and Baehrecke, 2004..

Acknowledgments

This work was supported by Fundação de Amparo à Pesquisa do Estado de São Paulo (2008/50036-3; 2005/54597-4); CNPq (Conselho Nacional de Desenvolvimento Científico e Tecnológico); Capes (Coordenação de Aperfeiçoamento de Pessoal de Nível Superior).

Appendix A. Supplementary data

Supplementary data related to this article can be found at <http://dx.doi.org/10.1016/j.asd.2014.05.001>.

References

- Aguila, J.R., Suszko, J., Gibbs, A.G., Hoshizaki, D.K., 2007. The role of larval fat cells in adult *Drosophila melanogaster*. *J. Exp. Biol.* 210 (6), 956–963.
- Akdemir, F., Farkaš, R., Chen, P., Juhasz, G., Medved'ová, L., Sass, M., Wang, L., Wang, X., Chittaranjan, S., Gorski, S.M., Rodriguez, A., Abrams, J.M., 2006. Autophagy occurs upstream or parallel to the apoptosome during histolytic cell death. *Development* 133 (8), 1457–1465.
- Araujo, R.V., Maciel, C., Hartfelder, K., Capurro, M.L., 2011. Effects of *Plasmodium gallinaceum* on hemolymph physiology of *Aedes aegypti* during parasite development. *J. Insect Physiol.* 57, 265–273.
- Baehrecke, E.H., 2003. Autophagic programmed cell death in *Drosophila*. *Cell. Death Differ.* 10 (9), 940–945.
- Basso, L.R., Vasconcelos, C., Fontes, A.M., Hartfelder, K., Silva Jr., J.A., Coelho, P.S.R., Monesi, N., Paço-Larson, M.L., 2002. The induction of DNA puff BhC4-1 gene is a late response to the increase in 20-hydroxyecdysone titers in last instar dipteran larvae. *Mech. Dev.* 110, 15–20.
- Berry, D.L., Baehrecke, E.H., 2007. Growth arrest and autophagy are required for salivary gland degradation in *Drosophila*. *Cell* 131 (6), 1137–1148.
- Berry, D.L., Baehrecke, E.H., 2008. Autophagy functions in programmed cell death. *Autophagy* 4 (3), 359–360.
- Bollenbacher, W.E., O'Brien, M.A., Katahira, E.J., Gilbert, L.I., 1983. A kinetic-analysis of the action of the insect prothoracicotropic hormone. *Mol. Cell. Endocrinol.* 32, 27–46.
- Borst, D.W., Bollenbacher, W.E., O'Connor, J.D., King, D.S., Fristrom, J.W., 1974. Ecdysone levels during metamorphosis of *Drosophila melanogaster*. *Dev. Biol.* 39, 308–316.
- Breuer, M.E., Pavan, C., 1955. Behavior of polytene chromosomes of *Rhynchosciara angelae* at different stages of larval development. *Chromosoma* 7, 371–386.
- Burry, R.W., 2000. Specificity controls for immunocytochemical methods. *J. Histochem. Cytochem.* 48 (2), 163–165.
- Chen, Y., Yu, L., 2013. Autophagic lysosome reformation. *Exp. Cell. Res.* 319 (2), 142–146.
- Cuervo, A.M., 2004. Autophagy: in sickness and in health. *Trends Cell. Biol.* 14 (2), 70–77.
- Denton, D., Shravage, B., Simin, R., Mills, K., Berry, D.L., Baehrecke, E.H., Kumar, S., 2009. Autophagy, not apoptosis, is essential for midgut cell death in *Drosophila*. *Curr. Biol.* 19 (20), 1741–1746.
- Denton, D., Shravage, B.V., Simin, R., Baehrecke, E.H., Kumar, S., 2010. Larval midgut destruction in *Drosophila*: not dependent on caspases but suppressed by the loss of autophagy. *Autophagy* 6 (1), 163–165.
- Feldlaufer, M.F., Hartfelder, K., 1997. Relationship of the neutral sterols and ecdysteroids of the parasitic mite, *Varroa jacobsoni* to those of the honey bee, *Apis mellifera*. *J. Insect Physiol.* 43, 541–545.
- Ge, L., Schenckman, R., 2014. The ER-Golgi intermediate compartment feeds the phagophore membrane. *Autophagy* 10 (1), 170–172.
- Gozuacik, D., Kimchi, A., 2004. Autophagy as a cell death and tumor suppressor mechanism. *Oncogene* 23 (16), 2891–2906.
- Hannigan, A.M., Gorski, S.M., 2009. Macroautophagy: the key ingredient to a healthy diet? *Autophagy* 5 (2), 140–151.
- Hodgetts, R.B., Sage, B., O'Connor, J.D., 1977. Ecdysone titers during postembryonic development of *Drosophila melanogaster*. *Dev. Biol.* 60, 310–317.
- Hou, Y.-C.C., Chittaranjan, S., Barbosa, S.G., McCall, K., Gorski, S.M., 2008. Effector caspase Dcp-1 and IAP protein Bruce regulate starvation-induced autophagy during *Drosophila melanogaster* oogenesis. *J. Cell. Biol.* 182 (6), 1127–1139.
- Jurand, A., Pavan, C., 1975. Ultrastructural aspects of histolytic processes in the salivary gland cells during metamorphic stages in *Rhynchosciara hollaenderi* (Diptera, Sciaridae). *Cell. Differ.* 4 (4), 219–236.
- Keeley, L.L., 1985. Biochemistry and physiology of the insect fat body. In: Kerkut, G.A., Gilbert, L.I. (Eds.), *Comprehensive Insect Physiology, Biochemistry and Pharmacology*, vol. 3. Pergamon, New York, pp. 211–228.
- Klionsky, D.J., 2009a. Crohn's disease, autophagy, and the paneth cell. *N. Engl. J. Med.* 360 (17), 1785–1786.
- Klionsky, D.J., 2009b. Crohn disease and autophagy. *Autophagy* 5 (2), 139.
- Lara, F.J.S., Tamaki, H., Pavan, C., 1965. Laboratory culture of *Rhynchosciara angelae*. *Am. Nat.* 99, 189–191.
- Law, J.H., Wells, M.A., 1989. Insects as biochemical models. *J. Biol. Chem.* 264, 16335–16338.
- Lee, C.Y., Baehrecke, E.H., 2001. Steroid regulation of programmed cell death during development. *Development* 128, 1443–1455.
- Levine, B., Yuan, J., 2005. Autophagy in cell death: an innocent convict? *J. Clin. Investig.* 115 (10), 2679–2688.
- Lindmo, K., Simonsen, A., Brech, A., Finley, K., Rusten, T.E., Stenmark, H., 2006. A dual function for deep orange in programmed autophagy in the *Drosophila melanogaster* fat body. *Exp. Cell. Res.* 312, 2018–2027.
- Liu, W.-T., Huang, C.-Y., Lu, I.-C., Gean, P.-W., 2013. Inhibition of glioma growth by minocycline is mediated through endoplasmic reticulum stress-induced apoptosis and autophagic cell death. *Neuro-Oncology*.
- Machado-Santelli, G.M., Basile, R., 1975. DNA replication and DNA puffs in salivary chromosomes of *Rhynchosciara*. *Ciência Cult.* 27, 167–174.
- Martin, D.N., Baehrecke, E.H., 2004. Caspases function in autophagic cell death in *Drosophila*. *Development* 131, 275–284.
- Martin, D.N., Balgley, B., Dutta, S., Chen, J., Rudnick, P., Cranford, J., Kantartzis, S., DeVoe, D.L., Lee, C., Baehrecke, E.H., 2007. Proteomic analysis of steroid-triggered autophagic programmed cell death during *Drosophila* development. *Cell. Death Differ.* 14 (5), 916–923.
- McPhee, C.K., Baehrecke, E.H., 2009. Autophagy in *Drosophila melanogaster*. *Biochim. Biophys. Acta (BBA) – Mol. Cell. Res.* 1793 (9), 1452–1460.
- McPhee, C.K., Balgley, B.M., Nelson, C., Hill, J.H., Batlevi, Y., Fang, X., Lee, C.S., Baehrecke, E.H., 2013. Identification of factors that function in *Drosophila* salivary gland cell death during development using proteomics. *Cell. Death Differ.* 20 (2), 218–225.
- Mizushima, N., 2007. Autophagy: process and function. *Genes. Dev.* 21 (22), 2861–2873.
- Myohara, M., 2004. Real-time observation of autophagic programmed cell death of *Drosophila* salivary glands in vitro. *Dev. Genes. Evol.* 214, 99–104.
- Nelliot, A., Bond, N., Hoshizaki, D.K., 2006. Fat-body remodeling in *Drosophila melanogaster*. *Genesis* 44, 396–400.
- Niemann, A., Takatsuki, A., Elsässer, H.-P., 2000. The Lysosomotropic agent monodansylcadaverine also acts as a solvent polarity probe. *J. Histochem. Cytochem.* 48 (2), 251–258.
- Niemann, A., Baltes, J., Elsässer, H.-P., 2001. Fluorescence properties and staining behavior of Monodansylpentane, a structural homologue of the Lysosomotropic agent Monodansylcadaverine. *J. Histochem. Cytochem.* 49 (2), 177–185.
- Nijhout, H.F., 1984. *Insect Hormones*. Princeton University Press, Princeton NJ, p. 267.
- Orme, M., Meier, P., 2009. Inhibitor of apoptosis proteins in *Drosophila*: gatekeepers of death. *Apoptosis* 14 (8), 950–960.
- Pavan, C., 1965. Nucleic acid metabolism in polytene chromosomes and the problem of differentiation. *Brookhaven Symposia Biol. (No18)*, 222–241.
- Pavan, C., Breuer, M., 1952. Polytene chromosomes in different tissues of *Rhynchosciara*. *J. Hered.* 63, 151–157.
- Qu, X., Zou, Z., Sun, Q., Luby-Phelps, K., Cheng, P., Hogan, R.N., Gilpin, C., Levine, B., 2007. Autophagy gene dependent clearance of apoptotic cells during embryonic development. *Cell* 128, 931–946.
- Rezende-Teixeira, P., Palomino, N.B., Machado-Santelli, G.M., 2012. Rananos expression pattern during oogenesis and early embryonic development in *Rhynchosciara americana*. *Dev. Genes. Evol.* 222 (3), 153–164.
- Riddiford, L.M., Hiruma, K., Zhou, X., Nelson, C.A., 2003. Insights into the molecular basis of the hormonal control of molting and metamorphosis from *Manduca sexta* and *Drosophila melanogaster*. *Insect Biochem. Mol. Biol.* 33, 1327–1338.
- Rubinsztein, D.C., Cuervo, A.M., Ravikumar, B., Sarkar, S., Korolchuk, V.I., Kaushik, S., Klionsky, D.J., 2009. In search of an "autophagometer". *Autophagy* 5 (5), 585–589.
- Santelli, R.V., Machado-Santelli, G.M., Pueyo, M.T., Navarro-Cattapan, L.D., Lara, F.J.S., 1991. Replication and transcription in the course of DNA amplification of the C3 and C8 DNA puffs of *Rhynchosciara americana*. *Mech. Dev.* 36 (1–2), 59–66.
- Santelli, R., Siviero, F., Machado-Santelli, G.M., Lara, F.J.S., Stocker, A., 2004. Molecular characterization of the B-2 DNA puff gene of *Rhynchosciara americana*. *Chromosoma* 113 (4), 167–176.
- Shibutan, S.T., Yoshimori, T., 2014. A current perspective of autophagosome biogenesis. *Cell. Res.* 24, 58–68.
- Siviero, F., Rezende-Teixeira, P., Andrade, A., Machado-Santelli, G.M., Santelli, R.V., 2006. Analysis of expressed sequence tags from *Rhynchosciara americana* salivary glands. *Insect Mol. Biol.* 15 (2), 109–118.
- Terra, W.R., De Bianchi, A.G., Gambarini, A.G., Lara, F.J.S., 1973. Haemolymph amino acids and related compounds during cocoon production by the larvae of the fly, *Rhynchosciara americana*. *J. Insect Physiol.* 19 (11), 2097–2106.

- Tian, L., Liu, S., Liu, H., Li, S., 2012. 20-Hydroxyecdysone upregulates apoptotic genes and induces apoptosis in the *Bombyx* fat body. *Arch. Insect Biochem. Physiol.* 79 (4–5), 207–219.
- Tracy, K., Baehrecke, E.H., 2013. Chapter four – the role of autophagy in Drosophila metamorphosis. In: Yun-Bo, S. (Ed.), *Current Topics in Developmental Biology*. Academic Press, pp. 101–125.
- Warren, J.T., Gilbert, L.I., 1986. Ecdysone metabolism and distribution during the pupal-adult development of *Manduca sexta*. *Insect Biochem.* 16, 65–82.
- Winter, C.E., De Bianchi, A.G., Terra, W.R., Lara, F.J.S., 1977a. Relationships between newly synthesized proteins and puff patterns in salivary glands of *Rhynchosciara americana*. *Chromosoma* 61, 193–206.
- Winter, C.E., De Bianchi, A.G., Terra, W.R., Lara, F.J.S., 1977b. The giant DNA puffs of *Rhynchosciara americana* code for polypeptides of the salivary gland secretion. *J. Insect Physiol.* 23 (11–12), 1455–1459.

UNCORRECTED PROOF